3 Biotech (2019) 9:86
https://doi.org/10.1007/s13205-019-1623-x

ORIGINAL ARTICLE

# Enhanced degradation of indeno(1,2,3-cd)pyrene using *Candida tropicalis* NN4 in presence of iron nanoparticles and produced biosurfactant: a statistical approach

**Nupur Ojha[1] · Sanjeeb Kumar Mandal[1] · Nilanjana Das[1]**

Received: 15 June 2018 / Accepted: 8 February 2019 / Published online: 15 February 2019


**Abstract**
Seven yeast isolates were screened for the remediation of indeno(1,2,3-cd)pyrene (InP) using biosynthesized iron nanoparticles and produced biosurfactant in growth medium. Four yeast isolates showed positive response to produce biosurfactant which was confirmed by drop collapse test, emulsification index, methylene blue agar plate method, oil displacement test and lipase activity. The yeast strain showing maximum potential for InP degradation and biosurfactant production was identified as *Candida tropicalis* NN4. The produced biosurfactant was characterized as sophorolipid type through TLC and FTIR analysis. Iron nanoparticles were biosynthesized using mint leaf extract and characterized by various instrumental analysis. Response surface methodology (RSM), three-level five-variable Box–Behnken design (BBD) was employed to optimize the factors, viz., pH (7), temperature (30 °C), salt concentration (1.5 g $L^{-1}$), incubation time (15 days) and iron nanoparticles concentration (0.02 g $L^{-1}$) for maximum InP degradation (90.68 ± 0.7%) using *C. tropicalis* NN4. It was well in close agreement with the predicted value which was obtained by RSM model (90.68 ± 0.4%) indicating the validity of the model. InP degradation was confirmed through FTIR and GC–MS analysis. A kinetic study demonstrated that InP degradation fitted first-order kinetic model. This is the first report on yeast-mediated nanobioremediation of InP and optimization of the whole process using RSM.

**Keywords** Indeno(1,2,3-cd)pyrene · *Candida tropicalis* NN4 · Biosurfactant · Iron nanoparticles · Nanobioremediation · Box-Behnken design (BBD)

## Introduction

Polycyclic aromatic hydrocarbons (PAHs) are a class of toxic environmental pollutants consisting of two or more fused benzene rings in various arrangements (Su et al. 2018). Indeno(1,2,3-cd)pyrene (InP), a polycyclic aromatic hydrocarbon (PAH) containing six fused benzene rings, is considered to be one of the 16 PAHs defined as a priority pollutant by the US EPA due to its high toxicity, mutagenic and carcinogenic nature (Lawal 2017; Ping et al. 2017a, b). For drinking water, WHO suggested a recommended limit of 200 ng $L^{-1}$ for (indeno(1,2,3-cd)pyrene) and the same limit has been adopted as an official maximum allowable concentration by the European Union (EU). The high molecular weight (HMW) PAHs with more than four rings are highly hydrophobic, minimally bioavailable, and more recalcitrant. Traditionally, their fate is associated with both abiotic and biotic factors which include volatilization, photo-oxidation, and adsorption to soil particles, chemical oxidation, and biological processes (Ping et al. 2017a, b).

The process of bioremediation defined as the use of microorganisms for detoxification or removal of pollutants, which relies upon microbial enzymatic activities to transform or degrade hazardous contaminants, has been greatly used in hydrocarbon mitigation since it is low-cost and highly efficient in converting pollutants to less-harmful or non-toxic end products (Mnif et al. 2017). Biodegradation

**Electronic supplementary material** The online version of this article (https://doi.org/10.1007/s13205-019-1623-x) contains supplementary material, which is available to authorized users.

✉ Nilanjana Das
nilanjanamitra@vit.ac.in

[1] Bioremediation Laboratory, Department of Biomedical Sciences, School of Bio Sciences and Technology, VIT (Vellore Institute of Technology), Vellore, Tamil Nadu 632014, India

has been proposed as one of the effective means to remediate PAHs from contaminated environments. A large number of PAHs degrading bacteria have been isolated, but reports are scanty in case of microorganisms as degrader of indeno(1,2,3-cd)pyrene (Huang et al. 2015; Du et al. 2010). Though yeasts are tolerant to changes in adverse environmental conditions (Ooi et al. 2003), reports are less on yeast as biodegrader of high molecular weight PAHs like InP (Bhattacharya et al. 2014).

Biosurfactants or microbial surface active agents are extracellular products consisting of hydrophobic and hydrophilic moieties which tend to interact with surfaces of different polarities. These surface agents are capable of reducing the surface and interfacial tension of solutions, facilitating hydrocarbon uptake as well as emulsification/dispersion. These can also improve the bioavailability of hydrocarbons to the microbial cells by increasing the area of contact at the aqueous–hydrocarbon interface which increases the rate of hydrocarbon dissolution and their utilization by microorganisms (Kumar et al. 2016). They are considered as best alternatives to chemical surfactants towards enhancing hydrocarbons solubility, bioavailability, and biodegradation (Mnif et al. 2017). Biosurfactant production and biosurfactant addition have been reported to enhance hydrocarbon assimilation (Kumar et al. 2016). Biosurfactants being the most versatile compounds have gained considerable attention for numerous industrial, medical and environmental applications including remediation of a number of pollutants (Ibrahim 2018).

The effect of nanoparticles on microorganisms has additionally attracted attention nowadays because of their unique impact on microbiological responses being located on the cells to stimulate the activity of microbes (Luo et al. 2015; Mueller-Spitz and Crawford 2014; Shin and Cha 2008; Muller et al. 2014; Zhang et al. 2017). The effect of produced biosurfactant and specific concentration of ($Fe_2O_3$ and $Zn_5OH_8Cl_2$) nanoparticles for remediation of crude oil has recently been reported by El-Sheshtawy and Ahmed (2017). This report highlighted the significance of using nanoparticles and biosurfactant for the remediation of high molecular weight hydrocarbons. However, no report is available on bioremediation of PAHs in presence of biosynthesized Fe nanoparticles and produced biosurfactant in the growth medium using microbes which have been the focus of our present study.

A large number of PAHs degrading microorganisms have been isolated, but reports are scanty in case of microorganisms as degrader of indeno(1,2,3-cd)pyrene (Huang et al. 2015; Du et al. 2010).

Response surface methodology (RSM), three-level three-variable Box–Behnken design (BBD) was employed to optimize the InP degradation process involving various factors such as pH, temperature, salt concentration, incubation time and iron nanoparticles concentration for maximum InP degradation. BBD is statistically more superior design for RSM which mathematically computes the importance of a large number of variables in less number of experiments.

The objectives of the present study include: (1) isolation and identification of yeast strain capable of degrading indeno(1,2,3-cd)pyrene (InP); (2) biodegradation of InP in presence of iron nanoparticles and produced biosurfactant in the growth medium and (3) statistical optimization of essential variables which could improve biodegradability of InP using response surface methodology (RSM).

## Materials and methods

### Isolation and screening of InP-degrading yeast

Industrial soil was collected from SIDCO Industrial Estate, Ranipet, Tamil Nadu, India. Yeast strains were isolated from the industrial soil by serial dilution and spread plating techniques on YEPD agar medium plates contained (g $L^{-1}$) yeast extract (10.0), peptone (20.0), dextrose (20.0) and agar (15.0) and incubated for 48 h at 30 °C. Isolated yeast strains were subcultured on YEPD medium and preserved at 4 °C for conducting further experiments. The screening of InP-degrading yeast strains was done by growing the isolated yeast strains in 100 ml of minimal salt medium (MSM) containing (g $L^{-1}$) $K_2HPO_4{\cdot}2H_2O$ (1.0), $KH_2PO_4$ (1.0), NaCl (5.0), $(NH_4)_2SO_4$ (3.0), $MgSO_4{\cdot}7H_2O$ (3.0), $CaCl_2$ (0.02) supplemented with InP (1 mg $L^{-1}$) as carbon source and incubated for 15 days at 30 °C under shaking condition (150 rpm). Their ability to tolerate InP was accessed by measuring the turbidity using colorimeter at 600 nm. MSM flask without InP was kept as control (Haghighat et al. 2008). Further, the InP degrading screened yeast strains were streaked on YEPD slants supplemented with InP (1 mg $L^{-1}$) incubated at 30 °C for 48 h and preserved at 4 °C for conducting further experiments.

### Culture media for biosurfactant production

For inoculum preparation, screened yeast strains were inoculated in 100-ml Erlenmeyer flask containing 50 ml of YEPD broth separately and were incubated inside a rotary shaker of 150 rpm at 30 °C for 12–24 h until cell numbers reached to $10^8$ CFU/ml. For biosurfactant production, a mineral salt medium (MSM) with the following composition of (g $L^{-1}$): $Na_2HPO_4$ (2.0), $KH_2PO_4$ (2.0), $MgSO_4{\cdot}7H_2O$ (0.01), $NaNO_3$ (2.5), NaCl (0.8) $CaCl_2$, (0.2), KCl (0.8), $FeSO_4{\cdot}7H_2O$, (0.001) supplemented with glucose (2%) w/v, yeast extract (3%) w/v, and 5 ml of trace element solution was prepared. Trace element solution contained (g $L^{-1}$): $FeSO_4{\cdot}7H_2O$ (0.116), $H_3BO_3$ (0.232), $CoCl_2.6H_2O$ (0.41), $CuSO_4.5H_2O$

(0.008), $MnSO_4 \cdot H_2O$ (0.008), $(NH_4)_6Mo_7O_2$ (0.02) and $ZnSO_4$ (0.174) (Haghighat et al. 2008). The yeast inoculums (3% v/v) were inoculated separately in 500-ml Erlenmeyer flasks containing 150 ml MSM medium of initial pH 7 and incubated at 30 °C for 4 days under shaking condition of 150 rpm to monitor the biosurfactant activities.

## Screening of biosurfactant-producing yeast

The screening of the yeast strains for biosurfactant production was done following different methods, viz., drop collapse test (Bodour and Miller-Maier 1998), methylene blue agar plate method (Satpute et al. 2008), oil displacement test, lipase activity test (Khopade et al. 2012) and emulsification test (E24) (Bodour et al. 2004). Based on the screening tests results, the yeast strain showing the maximum biosurfactant production was selected, identified at a molecular level and used for further experiments.

## Molecular identification of InP-degrading yeast

The InP-degrading yeast strain was subjected to the molecular identification via partial 18SrDNA sequencing, complete internal transcribed sequence (ITS) 1, 5.8S, ITS2, and Domain 1, Domain 2, Domain 3 region of large subunit (LSU) by Progen Biotech Limited, Tamil Nadu, India. The potent yeast strain was identified by amplifying 18S rDNA gene using universal primers ITS1 (5′TCC GTA GGT GAA CCTTGC GG 3′) and ITS4 (5′TCC TCC GCT TAT TGA TAT GC 3′). The 18Sr DNA gene sequence obtained from potent yeast isolate was compared with the neighbor yeast sequences through NCBI Mega BLAST for their pairwise identification and the sequence being novel was submitted to GenBank. The multiple alignments of these sequences were aligned using CLUSTAL-W software and the phylogenetic tree was represented using the neighbor-joining method with tree view software X.

## Biosurfactant production, purification, and characterization

For biosurfactant production, the screened yeast strain (3% v/v) was inoculated in 500-ml Erlenmeyer flasks containing 150 ml MSM medium of initial pH 7.0 and incubated at 30 °C for 4 days under shaking condition of 150 rpm to obtain highest cell and surfactant concentration (Chandran and Das 2012). For the extraction of biosurfactant, yeast culture broth was centrifuged at 10,000 rpm for 20 min to separate out the cell-free supernatant from the yeast cells. The cell-free supernatant was then precipitated by adding an equal volume of ice-cold acetone and mixed thoroughly to get the precipitate. The resulting white precipitate was collected by centrifugation at 5000 rpm for 15 min and dissolved in Milli-Q water and finally lyophilized to obtain the crude biosurfactant fractions (Satpute et al. 2010). The weight of the biosurfactant was expressed in terms of mg $mL^{-1}$ (dry weight).

The lyophilized biosurfactant was dissolved in chloroform and then purified by silica gel chromatography following the method of Thavasi et al. (2009). The crude residue was purified on a silica gel (60–120) mesh column eluting with a chloroform/methanol gradient ranging from 20:1 to 2:1, collecting ten fractions. Further, the fractions eluted were pooled and the solvents were evaporated. The resulting residue was dialyzed against distilled water and freeze-dried using lyophilizer.

Biochemical composition of the purified biosurfactant was analyzed following standard methods. The total carbohydrate content of the biosurfactant was determined by the anthrone reagent method (Spiro 1966). D-Glucose was used as a standard. Lipid content was estimated following the standard procedure of Folch et al. (1957). Protein content was determined using bovine serum albumin as a standard following the method of Lowry et al. (1951).

Structural characterization of purified biosurfactant was done by Fourier transform infrared spectroscopy (FTIR). For FTIR analysis, 1 mg of lyophilized purified biosurfactant was ground with 100 mg of KBr and pressed with 7500 kg for 30 s to obtain translucent pellets. The infrared spectra were recorded on FTIR system within the range of 500–4000 $cm^{-1}$ wave number.

## Biosynthesis and characterization of iron (Fe) nanoparticles

The iron nanoparticles were synthesized using an extract of fresh mint leaves. The mint plant leaves (5 g) were washed thoroughly with distilled water and cut into fine pieces and were subsequently macerated in 50-ml mixture of double distilled water and methanol (1:1). This liquefied mixture was subjected to centrifugation at 10,000 rpm for 5 min at 4 °C and the supernatant was separated out. The supernatant obtained was used as a reductant for the synthesis of the iron nanoparticles. For the synthesis of Fe nanoparticles, mint leaf extract (5 ml) was added dropwise into the solution of ferric nitrate (10 mM) under magnetic stirring condition. Later the content was placed on to a rotatory orbital shaker operating at 200 rpm for 72 h at 30 °C under dark condition (Prasad et al. 2014). The reduction of iron ions was monitored at intervals of 24 h followed by measurement of the UV–Vis spectra using a spectrophotometer. A spectral scanning analysis was carried out to find the maximum absorption by measuring the optical density of the sample after 72 h using UV–Vis spectrophotometer from wavelength 300–700 nm (Devatha et al. 2016).

The synthesized iron nanoparticles were extracted after 72 h of incubation by centrifuging the sample at 13,000 rpm

for 10 min. The recovered pellet was then washed with 50 ml of 1:1, methanol–water solution for removing the organic impurities and pellet was freeze-dried using a lyophilizer. The dried pellet of synthesized nanoparticles was ground into powder form and subjected to elemental analysis using X-ray diffraction (XRD) and Fourier-transform infrared spectroscopy (FTIR) analysis following the standard method as demonstrated by Prasad et al. (2014).

The TEM analysis of the synthesized Fe nanoparticles was done using JEOL 2100 HRTEM instrument from a great accelerating voltage of 200 kV. The fine powdered form of Fe nanoparticles was dispersed in ethanol by ultra-sonication and the sample was mounted on a micro-grid carbon film supported on a copper grid by placing a few droplets of a suspension followed by drying at 25 °C (El-Sheshtawy and Ahmed 2017).

## Biodegradation of InP in presence of Fe nanoparticles and produced biosurfactant

The biodegradation experiments were conducted in sterilized 250-ml Erlenmeyer flask containing 100 ml of mineral salt medium supplemented by InP (1 mg $L^{-1}$) under different set of conditions as follows: (i) InP + Isolate 4, (ii) InP + Isolate 4 + produced biosurfactant, (iii) InP + Isolate 4 + Fe nanoparticles (0.008 g $L^{-1}$), (iv) InP + Isolate 4 + produced biosurfactant + Fe nanoparticles (0.008 g $L^{-1}$). The medium without yeast inoculation was maintained as a control. For the extraction of residual InP, the yeast culture broths incubated under different sets of conditions were collected after 15 days of biodegradation process and centrifuged at 8000 rpm for 20 min. The supernatant was collected to remove residual crystalline InP. Further, the pH of the supernatant was adjusted to 2.0 after addition of 2 N HCl and sodium chloride (20%, w/v) to obtain better separation of the aqueous and organic layers. The extracts were taken twice using equal volumes of ethyl acetate. The solvents were removed under vacuum by rotary evaporation (Superfit™ Rotary vacuum Digital bath) until a constant weight was attained. The extracted InP samples from the different set of conditions was accurately weighed after 15 days of incubation and the percentage of the biodegraded InP was determined gravimetrically using the formula as follows:

$$\text{InP degradation}\,(\%) = C_i - C_f/C_i \times 100,$$

where $C_i$ is the initial concentration of InP introduced in the medium and $C_f$ is the final concentration of InP remaining in the medium.

## Instrumental analysis

The residual InP and its degraded products along with the respective control samples were analyzed using gas chromatography–mass spectrometric analysis (GC–MS) after 15 days of the biodegradation process. The biodegradation of InP was monitored through a JEOL GC MATEII gas chromatographic instrument. The component separation was performed using Elite55MS column (silica gel, 30 m length, 0.25 µm diameter). The inlet temperature was 100–300 °C with a fixed rate associated with 3 °C $min^{-1}$. Helium was used as carrier gas for the whole separation at a flow rate of 1.0 mL/min. The chromatogram of pure InP obtained through GC–MS analysis was used as standard chromatogram against the different sets of conditions, viz., (i) InP + Isolate 4, (ii) InP + Isolate 4 + produced biosurfactant, (iii) InP + Isolate 4 + Fe nanoparticles (0.008 g $L^{-1}$), (iv) InP + Isolate 4 + produced biosurfactant + Fe nanoparticles (0.008 g $L^{-1}$) and control samples (Sigma Aldrich). The obtained chromatograms of the extracted residual InP incubated under different sets of conditions were compared with respective spectra of authentic compounds present in the standard chromatogram and also with the mass profile of the same compound available in the National Institute of Standard Technology (NIST) library, USA (Boz et al. 2009).

The FTIR spectra of InP degraded products were used to determine the vibrational frequency changes in the functional groups. IR spectroscopy was investigated with an IR affinity$^{-1}$ FTIR spectrophotometer (Shimadzu) using KBr pellets. The range of scanning was kept between 4000 and 400 wavenumbers ($cm^{-1}$) with a resolution of 2 wave numbers per wave (Korda et al. 1997).

## Process optimization using Box–Behnken design (BBD)

Response surface methodology (RSM) using BBD was used to optimize the various parameters, viz., pH, temperature, incubation time, salt concentration and Fe nanoparticles concentrations for enhancing InP degradation using potent yeast strain. The quadratic model was used to analyze the data. Each factor in the design was studied at three different levels (− 1, 0, + 1) and the minimum and maximum ranges of pH, temperature, incubation time, salt concentration and Fe nanoparticles variables were determined as shown in supplementary file Table S1. A design of 46 experiments was formulated and experiments were carried out in 250-ml Erlenmeyer flasks containing 100 ml of production medium (InP 1 mg $L^{-1}$) with different concentrations of pH, temperature, incubation time, salt concentration and Fe nanoparticles concentrations and inoculated with 3% (v/v) of yeast inoculum under shaking condition (150 rpm). InP degradation was used as dependent variables as a response. The 3D contour plots were prepared to evaluate the optimized parameters, which influence the response. The respective responses were analyzed using a second-order polynomial equation, and the data were fitted to the equation by multiple

regression procedures. Later, an experiment was conducted in triplicates using the optimum values for variables given by response surface optimization to validate the predicted value and the observed value of the responses. The results of the experimental design were analyzed and interpreted using Design-Expert version 11.0 (Stat-Ease Inc. Minneapolis, MN, USA) statistical software (Sahoo and Gupta 2012).

### Kinetics of InP degradation

Degradation kinetics was performed in triplicates. The zero-order (Jianlong et al. 2002), first-order (Agarry et al. 2013) and second-order (Capellos and Bielski 1972) kinetic models were used to define the degradation of InP in mineral medium.

## Results and discussion

### Isolation and screening of InP-degrading yeast

Seven morphologically distinct yeast strains were isolated from industrial soil and subcultured on YEPD agar plates. The yeast isolates, viz., Isolate 1, Isolate 2, Isolate 4 and Isolate 6 showed growth in the aqueous medium containing InP (1 mg $L^{-1}$) as shown in supplementary file Table S2. This indicated that screened yeast isolates had the potentiality to tolerate InP and utilize it as a carbon and energy source.

### Screening of biosurfactant-producing yeast

Biosurfactant produced by screened yeast strains in the MS medium supplemented with trace elements was examined by drop collapse test, methylene blue agar, oil displacement, lipase activity and emulsification test. The positive results of all the tests confirmed the biosurfactant-producing ability of yeast isolates as shown in supplementary file Table S2. The flat drop appearance in microtitre plate indicated the positive results for drop collapse test. A dark blue halo zone in the methylene blue agar plate supplemented with cetyltrimethylammonium bromide indicated the ability to produce anionic biosurfactant by the yeast strains. A clear zone in oil displacement test and clear halos of lipolysis on tributyrin agar were observed in the case of Isolate 4. Among all the yeast isolates, maximum emulsification index (%) was found to be 69.9% by Isolate 4 which was selected for molecular identification and conducting further experiments.

### Molecular identification of InP-degrading yeast

The 18Sr DNA gene sequence obtained from yeast Isolate 4 was compared with the other yeast sequences using NCBI Mega BLAST for their pairwise identification and the sequence being novel was submitted to GenBank. According to the phylogenetic analysis, the nucleotide sequence of the DNA fragment encoding the 18SrDNA gene, small subunit ribosomal RNA, partial sequence; internal transcribed spacer 1, 5.8S ribosomal RNA gene, and internal transcribed spacer 2, complete sequence; and large subunit ribosomal RNA gene of yeast isolate NN4, clearly demonstrated that the closest matches belonged to the genus *Candida tropicalis* with the highest identity (99%) to *C. tropicalis* strain NITCSK13 (GenBank: KX198669.1). The multiple alignments of these sequences were aligned using CLUSTAL-W software and the phylogenetic tree was represented using the neighbor-joining method with tree view software X as shown in Fig. 1. The yeast strain NN4 was identified as *C.*

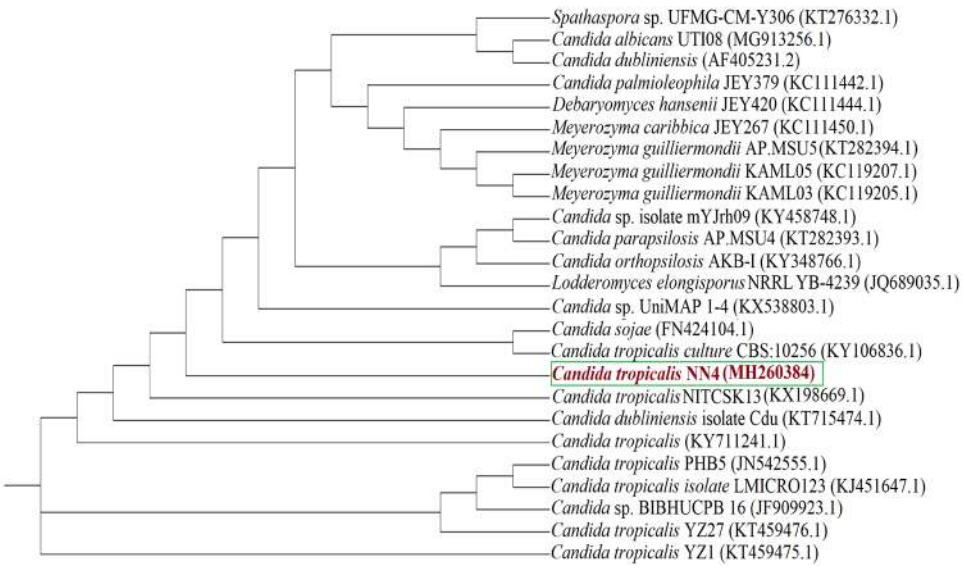


**Fig. 1** Phylogenetic tree of *Candida tropicalis* NN4 (MH260384) based on partial 18sRDNA, ITS1 complete, 5.8S complete ITS2 complete and D1, D2, a D3 region of LSU with its closest neighbors using tree view software

*tropicalis* sp. and named as *C. tropicalis* NN4 bearing accession number (MH260384).

## Purification and characterization of biosurfactant

The crude biosurfactant was extracted from the production medium using ice-cold acetone precipitation method and gave a maximum yield of 10 mg m $L^{-1}$. Further extracted crude biosurfactant was lyophilized, purified by silica gel column chromatography and visualized by TLC as shown in supplementary file Fig. S1. After charring the TLC plate at 110 °C, brown spots were formed indicating the presence of glycolipids which was further confirmed by compositional and structural characterization. The purified biosurfactant was characterized as glycolipid with total carbohydrate (47.56%) and lipid (59.32%) as major constituents. The absence of protein moiety confirmed the glycolipid nature of the biosurfactant.

The glycolipid nature of purified biosurfactant was further confirmed by the IR spectra of the compound. The FTIR spectrum of the purified freeze-dried biosurfactant produced by *C. tropicalis* NN4 is shown in Fig. 2. The FTIR spectrum exhibited absorption bands at 3601–3176 $cm^{-1}$ were corresponding to the O–H stretch of free hydroxyl alcohol. The absorption band at 3007.02 $cm^{-1}$ resembled the asymmetrical C–H stretching of the alkene. The absorption bands at 2926 and 2854 $cm^{-1}$ were corresponding to the C–H stretch of alkanes. The bands at 1745.58 and 1710.86 $cm^{-1}$ resembled the C=O stretch of carbonyl groups in acids and unsaturated lactones. The absorption band at 1658.78 $cm^{-1}$ was corresponding to the C=C stretch of alkenes. The stretch of a C–O band of alkanes appeared at 1462.04 $cm^{-1}$. The absorption bands of closed rings (C–C stretch) and ester linkages (C–O stretch) in sugars appeared at 1402.25 and 1075.35 $cm^{-1}$, respectively. Involvement of similar functional groups was reported by Mantsch and Chapman (1996). The small peaks at 887.26 and 717.52 $cm^{-1}$ were corresponding to C–H bend and C–H rock in a long linear aliphatic chain and acetyl groups which are common in compounds with lipid moiety. Production of sophorolipid biosurfactant by *C. tropicalis* was also reported by Chandran and Das (2012). No absorption peaks corresponding to peptides were observed in the FTIR spectrum of purified biosurfactant. Thus, the extracted and purified biosurfactant fractions by *C. tropicalis* NN4 was confirmed as sophorolipid biosurfactant type containing surface active glycolipid compound.

## Biosynthesis and characterization of iron (Fe) nanoparticles

The change in color from light brown to dark brown of the leaf extract containing ferric nitrate mixture indicated the reduction of iron ions into iron nanoparticles by the supernatant after 72 h of the incubation period. UV spectrum of the mixture after 72 h of incubation exhibited maximum absorption at two different wavelengths of 360 nm and 430 nm which clearly indicated the gradual formation of Fe nanoparticles during the incubation period as shown in Fig. 3a. Awwad and Salem (2012) reported carob

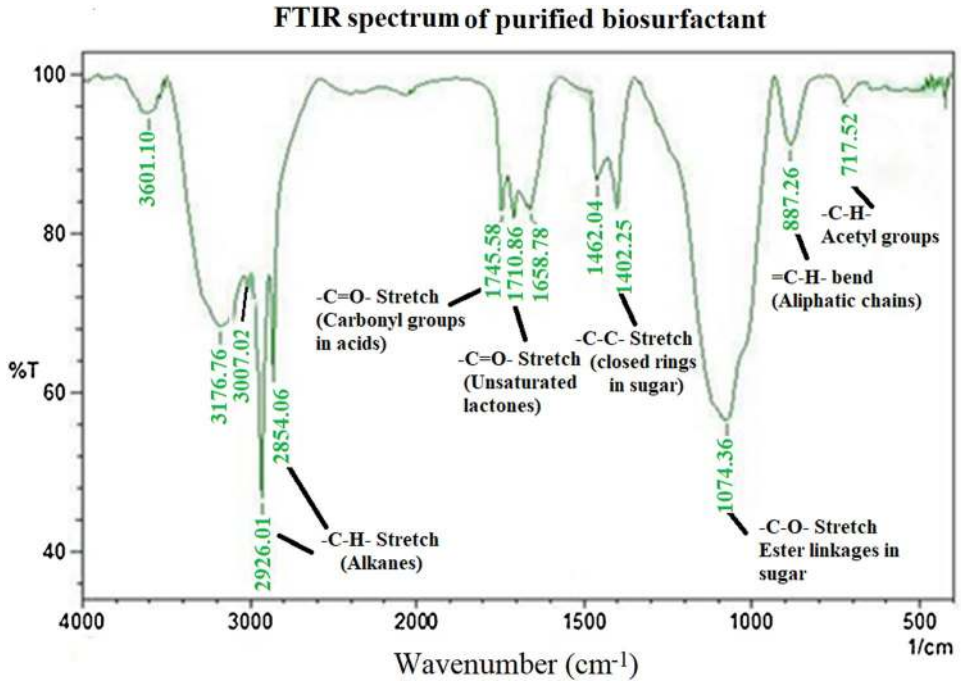


**Fig. 2** Characterization of the biosurfactant produced by *C. tropicalis* NN4 through FTIR analysis

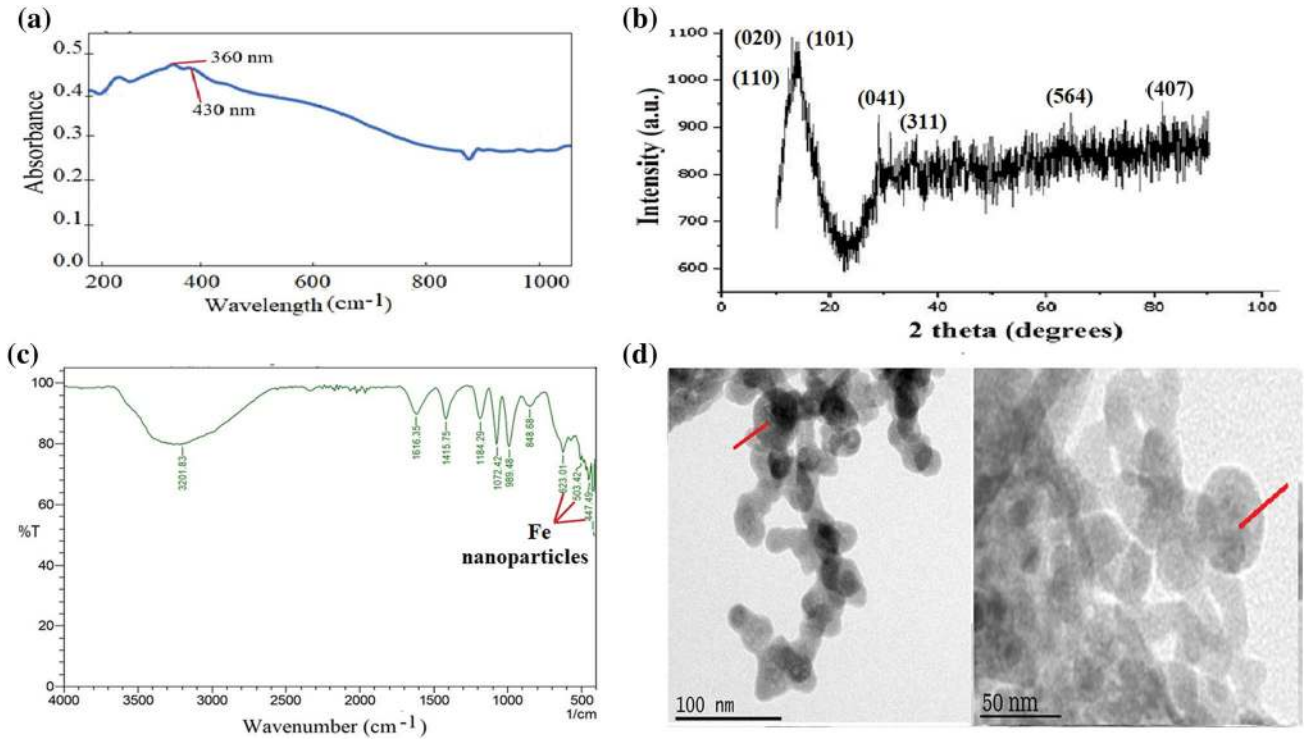


**Fig. 3** Characterization of iron nanoparticles. **a** UV–visible spectrophotometry analysis of Fe nanoparticles. **b** XRD analysis of synthesized Fe nanoparticles. **c** FTIR analysis of synthesized Fe nanoparticle. **d** TEM images of the synthesized Fe nanoparticles

leaf extract mediated synthesis of magnetic nanoparticles showed absorption maximum at 233 nm while Klačanová et al. (2013) demonstrated amino acid capped Fe° nanoparticles exhibited maximum absorption at 262, 369 and 430 nm, respectively. Similar results on the biosynthesis of Fe nanoparticles using leaf extract were reported by Wang et al. (2014) and Devatha et al. (2016).

The X-ray diffractogram of Fe nanoparticles exhibited well-defined peaks at 2$\theta$ values of 12.34, 12.97, 13.997, 29.05, 36.08, 64.54 and 81.41 which correspond to the 110, 020, 101, 041, 311, 564 and 407 planes, respectively. The intensity of Fe nanoparticles peaks at 2$\theta$ values of 13.997, 29.05, 36.08, 64.54 and 81.41 reflected the high degree of crystallinity in Fe nanoparticles which were in good agreement to the result reported by Prasad et al. (2014) as shown in Fig. 3b.

The FTIR spectrum of dispersed Fe nanoparticles in deionized water is shown in Fig. 3c. The peaks at 3414.89 $cm^{-1}$ are due to O–H stretching vibration arising from hydroxyl groups from the water on the nanoparticles. The absorption peaks at 1616.35, 1415.75, 1184.29 and 1072.42, 989 $cm^{-1}$ were due to de-ionized water used as a solvent. The absorption peaks at 623.01.29, 503.42 and 447.49 $cm^{-1}$ corresponded to the Fe bond vibration of Fe nanoparticles. A similar result was demonstrated by Chaki et al. (2015).

The surface morphological characteristics and size of the synthesized Fe nanoparticles were illustrated in the TEM images as shown in Fig. 3d. The TEM micrograph illustrated that the synthesized Fe nanoparticles by leaf extract exhibited spherical nanostructures with the average core diameter of 50 nm and the particles were seen to be agglomerated. Similar results of TEM analysis were reported where electron-dense spherical iron oxide particles having diameter ranging from 30 to 40 nm were synthesized using *Hordeum vulgare* extracts and *Rumex acetosa* extracts (Makarov et al. 2014).

## GC–MS analysis of InP degradation

The biodegradation studies of InP under different set of conditions, viz., (i) InP + *C. tropicalis* NN4, (ii) InP + *C. tropicalis* NN4 + produced biosurfactant, (iii) InP + *C. tropicalis* NN4 + Fe nanoparticles (0.008 g $L^{-1}$) and (iv) InP + *C. tropicalis* NN4 + produced biosurfactant + Fe nanoparticles (0.008 g $L^{-1}$) were analyzed through GC–MS analysis after 15 days of incubation. The respective chromatograms of the extracted residual InP incubated under different sets of conditions were compared with the standard (control) chromatogram and the degraded products produced during the biodegradation process were detected based on the retention time of the exhibited peaks as shown in Fig. 4a. The

standard chromatogram showed a major peak of InP at a retention time of 27.82 min. The reduction in the intensity of the peak exhibited at retention time 27.82 min was observed in all the respective chromatograms of condition (i), (ii) and (iii) with InP degradation of 61 ± 0.04%, 65 ± 0.02% and 75 ± 0.07%, respectively. However, the maximum reduction in the intensity of the InP peak was observed in the chromatogram of condition (iv), where the 79 ± 0.05% InP degradation by *C. tropicalis* NN4 in the presence of biosurfactant and nanoparticles was noted. Despite of InP peak at 27.82 min, other metabolite peaks at retention time 19.73 and 15.2 min in chromatogram (i), 25.7, 18.48 and 14.47 min in chromatogram (ii) and peaks at 13.03, 18.06 and 23.24 in chromatogram (iii) were also noted which indicated that InP was degraded into 2 or 1 benzene ring metabolites and long-chain fatty acids such as naphthalene,

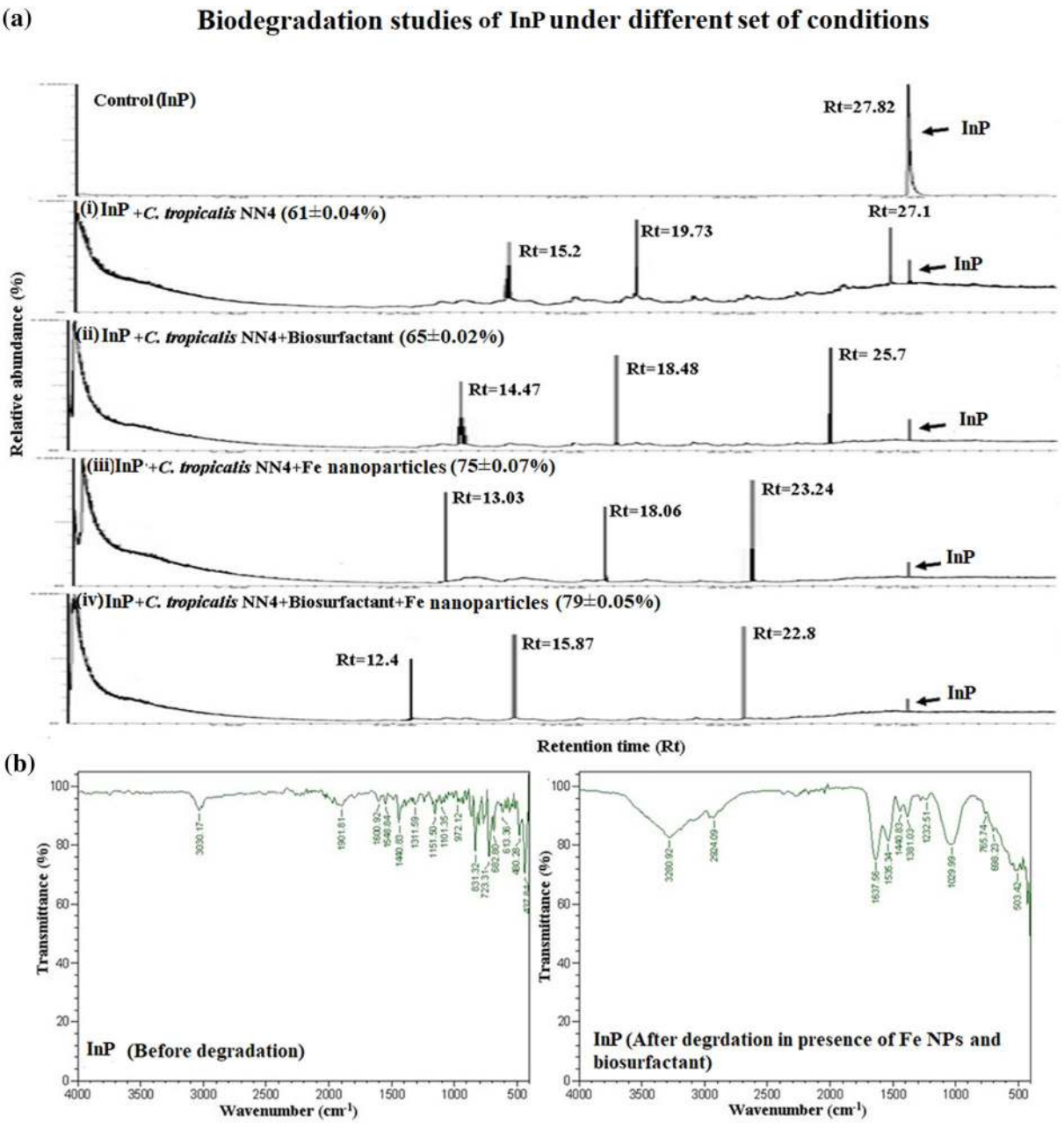


**Fig. 4** Biodegradation studies of InP degradation through instrumental analysis. **a** GC–MS analysis of residual InP treated under different set of conditions: (i) InP + *C. tropicalis* NN4, (ii) InP + *C. tropicalis* NN4 + produced biosurfactant, (iii) InP + *C. tropicalis* NN4 + Fe nanoparticles and (iv) InP + *C. tropicalis* NN4 + produced biosurfactant + Fe nanoparticles. **b** FTIR analysis

1,2-quinone and salicylic acid, respectively. The chromatogram of condition (iv), exhibited peaks at retention time 12.4, 15.87 and 22.8 min which indicated that addition of nanoparticles and biosurfactant had significantly improved the potentiality of the yeast *C. tropicalis* NN4 towards degradation of InP-forming products such as 3-hydroxyl decanoic acid, 3-methyl octadecanoic acid, methyl hexadecanoate. Thus, significant improvement in InP degradation (79 ± 0.05%) using *C. tropicalis* NN4 was noted when MSM was supplemented with biosurfactant and Fe nanoparticles (0.008 g $L^{-1}$). Du et al. (2010) reported 60% InP degradation using bacteria *Pandoraea* sp. after 25 days of incubation. Moreover, Huang et al. (2015) showed 87.9% InP degradation using immobilized bacterial cells in the soil after 40 days of incubation. Therefore, in the present study, the presence of Fe nanoparticles and produced biosurfactant in the medium showed a remarkable increase in the InP degradation (61 ± 0.04–79 ± 0.05%) using *C. tropicalis* NN4 only after 15 days of incubation.

## FTIR analysis of InP degradation

The FTIR spectrum of pure indeno(1,2,3-cd)pyrene exhibited distinctive absorption peaks at 3030.17 $cm^{-1}$ and 1901.81 $cm^{-1}$ corresponded C–H stretch in aromatic rings and weak overtone and combination bands in aromatic compounds, respectively. The prominent peaks at 1600.92, 1548.48, 1440.83 and 972.12 $cm^{-1}$ resembled the aromatic ring stretching and ring breathing mode of carbon ring in cyclic compounds, respectively. The absorption peaks at 831.32, 732.31, 682.80, 480.28 and 437.84 $cm^{-1}$ corresponded to strong CH deformations and medium–strong ring deformations in aromatic compounds as shown in Fig. 4b. The second FTIR spectrum illustrated, degraded indeno(1,2,3-cd)pyrene products by *C. tropicalis* NN4 in presence of Fe nanoparticles and biosurfactant after 15 days of incubation. This spectrum exhibited absorption peaks at 3280.92 and 2924.09 $cm^{-1}$ representing H-bonded OH stretch in the carboxylic acid. The sharp absorption peak at 1637.56 $cm^{-1}$ resembled C=C stretch in alkenes. The absorption peaks at 1535.34 and 1440.83 $cm^{-1}$ were corresponding to strong CH deformations in aromatic compounds. The absorption peaks at 1381.03 and 1232.51 $cm^{-1}$ resembled C–OH plan bending in alcohols and C–O–C stretch in ethers and esters (Fig. 4b). The peak at 1029.99 $cm^{-1}$ resembled ring breathing mode of carbon ring in cyclic compounds. The small absorption peaks at 765.74, 698.23 and 503.42 $cm^{-1}$ were corresponding to CH deformations as well as in medium–strong ring deformations in aromatic compounds. These results suggest that the parental compound has undergone significant changes after degradation.

## Process optimization using BBD

A three-level Box–Behnken design with six central points was used to enhance the InP biodegradation using yeast *C. tropicalis* NN4. Maximum InP biodegradation using *C. tropicalis* NN4 was found to be 90.68 ± 0.7 (%) at central values of all the factors, viz., pH (7.0), temperature (30 °C), incubation time (days), salt concentration (1.5 g $L^{-1}$) and Fe nanoparticles (0.02 g $L^{-1}$). *F* value of 75.07, $R^2$ of 0.9836, a probability of < 0.0001 and coefficient of variation of 1.97% confirmed that the model is highly significant and the experiments are accurate and reliable. An adequate precision of 32.68 for response also validates the model. The lack of fit analysis was found to be not significant in the present case shown in Table 1. Based on statistical significance, the second-order polynomial equation for the response can be written as:

$$\begin{aligned} Y = {} & 90.6833 + 4.1875 * A + 2 * B + 1.5 * C + -0.125 * D + 1.3125 * E + 0.5 * AB \\ & + 1.5 * AC + 2.5 * AD + 0.25 * AE + 1.5 * BC + -0.5 * BD + -1 * BE + 0.5 * CD \\ & + 1.2076e - 15 * CE + 1.5 * DE + -15.4042 * A^2 + -9.9875 * B^2 \\ & + -2.82083 * C^2 + -3.15417 * D^2 + -3.40417 * E^2, \end{aligned}$$

where *Y* represents InP biodegradation (%) as response and *A, B, C, D*, and *E* are coded terms for the five test variables, viz., pH, temperature, incubation time, salt and Fe nanoparticles concentration, respectively. The 3D and contour plots showed a significant influence on the response using *C. tropicalis* NN4 either independently or in interaction with each other (Fig. 5). Among all, *A, B, C, E, AC, AD, BC, DE,* $A^2$, $B^2$, $C^2$, $D^2$, and $E^2$ were found to be significant model terms ($p < 0.05$) as shown in Table 1. The interaction between the variables pH vs incubation time (*AC*), pH vs salt concentration (*AD*) and temperature vs incubation time (*BC*) had shown maximum InP degradation (90%) at neutral pH 7 at temperature of 30 °C with 1.5 g $L^{-1}$ salt concentration after 15 days of incubation (Fig. 5a–c). There was a report on 60% InP (1 mg $L^{-1}$) degradation using bacteria *Pandoraea* sp. (Du et al. 2010). The 3D and contour plots showed a significant impact of the variables salt concentration and Fe nanoparticles (DE) on InP degradation using *C. tropicalis* NN4 ($p < 0.05$) as shown in Fig. 5d. The maximum InP biodegradation (90%) was observed at a concentration of 0.02 g $L^{-1}$ Fe nanoparticles. The reduction in the InP degradation was noted at a higher concentration of

**Table 1** ANOVA for response surface quadratic model (response): InP degradation (%)

| Source | Sum of squares | *df* | Mean square | *F* value | *p* value |
|---|---|---|---|---|---|
| Model | 2973.65 | 20 | 148.68 | 75.07 | < 0.0001*** |
| *A*—pH | 280.56 | 1 | 280.56 | 141.66 | < 0.0001*** |
| *B*—temperature | 64.00 | 1 | 64.00 | 32.32 | < 0.0001 |
| *C*—incubation time | 36.00 | 1 | 36.00 | 18.18 | 0.0003** |
| *D*—salt (NaCl) | 0.25 | 1 | 0.25 | 0.13 | 0.7254 |
| *E*—Fe nanoparticles | 27.56 | 1 | 27.56 | 13.92 | 0.0010** |
| *AB* | 1.00 | 1 | 1.00 | 0.50 | 0.4839 |
| *AC* | 9.00 | 1 | 9.00 | 4.54 | 0.0430** |
| *AD* | 25.00 | 1 | 25.00 | 12.62 | 0.0015** |
| *AE* | 0.25 | 1 | 0.25 | 0.13 | 0.7254 |
| *BC* | 9.00 | 1 | 9.00 | 4.54 | 0.0430** |
| *BD* | 1.00 | 1 | 1.00 | 0.50 | 0.4839 |
| *BE* | 4.00 | 1 | 4.00 | 2.02 | 0.1676 |
| *CD* | 1.00 | 1 | 1.00 | 0.50 | 0.4839 |
| *CE* | 0.00 | 1 | 0.00 | 0.00 | 1.0000 |
| *DE* | 9.00 | 1 | 9.00 | 4.54 | 0.0430** |
| $A^2$ | 2070.88 | 1 | 2070.88 | 1045.65 | < 0.0001*** |
| $B^2$ | 870.55 | 1 | 870.55 | 439.57 | < 0.0001*** |
| $C^2$ | 69.44 | 1 | 69.44 | 35.06 | < 0.0001*** |
| $D^2$ | 86.83 | 1 | 86.83 | 43.84 | < 0.0001*** |
| $E^2$ | 101.13 | 1 | 101.13 | 51.07 | < 0.0001*** |
| Residual | 49.51 | 25 | 1.98 | | |
| Lack of fit | 46.58 | 20 | 2.33 | 3.98 | 0.0659NS |
| Pure error | 2.93 | 5 | 0.58 | | |
| Cor total | 3023.16 | 45 | | | |
| Std. dev. | 1.41 | | | | |
| Mean | 78.59 | | | | |
| C.V. % | 1.79 | | | | |
| $R^2$ | 0.98 | | | | |
| Adjusted $R^2$ | 0.97 | | | | |
| Predicted $R^2$ | 0.94 | | | | |
| Adeq precision | 32.68 | | | | |

**Significant, ***most significant, *NS* not significant

Fe nanoparticles which indicated that extreme concentration of Fe nanoparticles was toxic to yeast cell growth and resulted in the reduction of InP degradation. There are very few reports on the degradation studies of pollutants using nanoparticles in presence of produced biosurfactant in the growth medium. El-Sheshtawy and Ahmed (2017) reported crude oil degradation using *Bacillus licheniformis* in presence of produced biosurfactant in the medium and specific concentration of ($Fe_2O_3$ and $Zn_5OH_8C_{12}$) nanoparticles. So far Huang et al. (2015) reported 87.9% of indeno(1,2,3-cd) pyrene degradation in reed rhizosphere soil using microorganisms immobilized on cinder beads under natural environmental condition after 40 days of incubation; whereas, the present study had shown 90.68% of indeno(1,2,3-cd)pyrene degradation using *C. tropicalis* NN4 after 15 days of incubation in an aqueous medium in presence of Fe nanoparticles and produced biosurfactant under optimized conditions which shows the novelty of the present work.

In order to check the accuracy of the optimization, the model was validated by conducting the degradation experiment of InP using *C. tropicalis* NN4 in a batch reactor under optimum conditions of all the five variables *A, B, C, D*, and *E*. The experimental degradation percentage of InP was found to be 90.68 ± 0.7%, which was in good agreement with the predicted result 90.68 ± 0.4% indicating the validity of the model as shown in supplementary file Table S3. Hence the optimum point determined by RSM was successfully validated and it was confirmed that RSM can be used to optimize the degradation process of InP using *C. tropicalis* NN4 in presence of Fe nanoparticles and produced biosurfactant. The normal plot for residuals and predicted vs actual plots are represented in Fig. 5e, f, respectively. Thus,

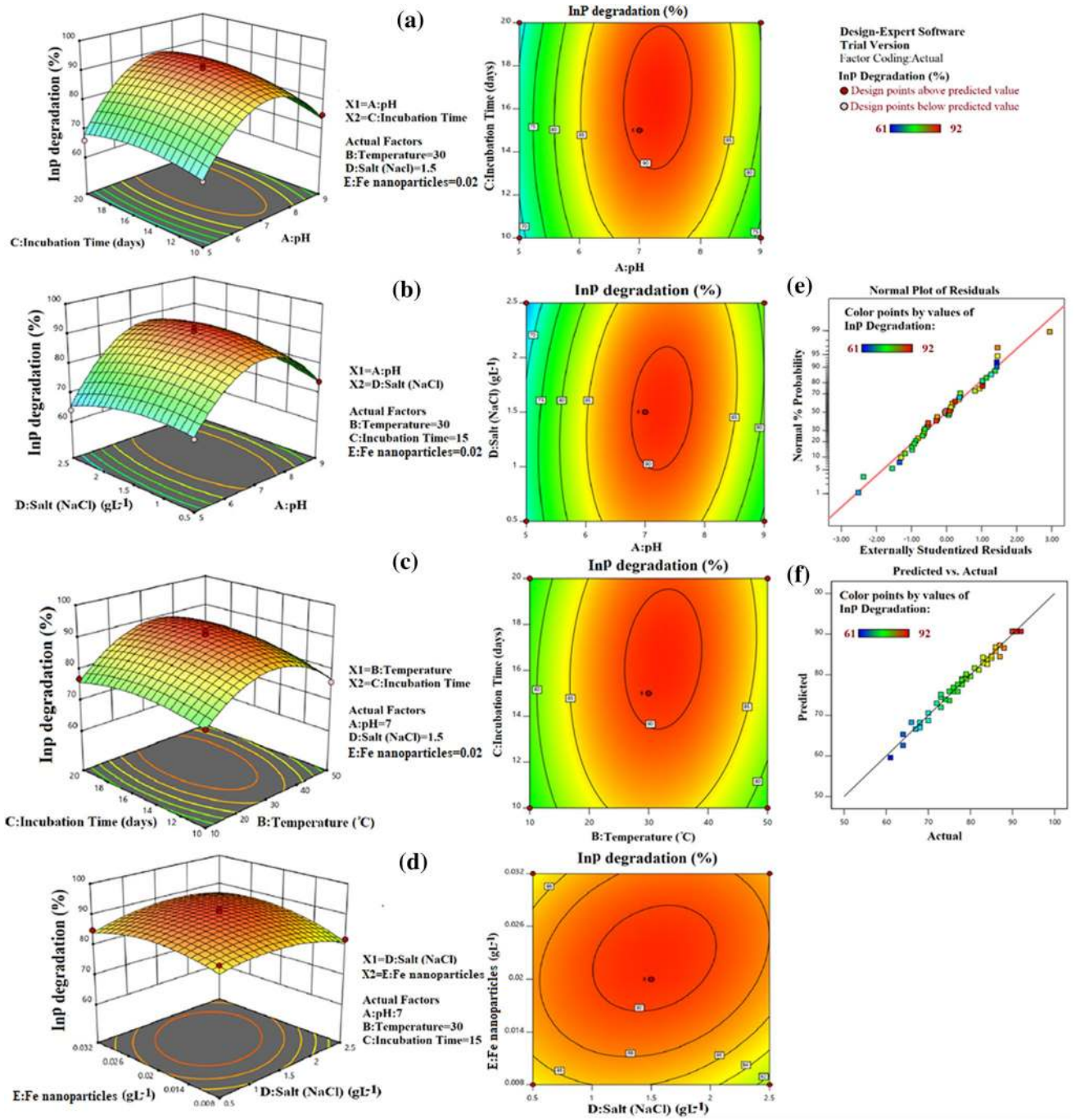


**Fig. 5** Process optimization of growth parameters for response: InP degradation (%) using BBD. 3-D and contour response plots representing the interactions between different variables and its significant effect on InP degradation. **a** Interaction between pH vs incubation time (*AC*). **b** Interaction between pH vs salt concentration (*AD*). **c** Interaction between temperature vs incubation time (*BC*). **d** Interaction between temperature vs salt concentration (*BD*). **e** Normal plot of residuals. **f** Predicted vs actual plot

a remarkable increase from 79.0 to 90.68% in the InP biodegradation using *C. tropicalis* NN4 was observed in the aqueous medium under optimized conditions of pH (7) at temperature (30 °C) after 15 days of incubation time, supplemented with 1.5 g $L^{-1}$ of salt and in presence of iron nanoparticles (0.02 g $L^{-1}$).

**Table 2** Kinetic studies for the biodegradation of InP under different set of conditions

| Set of conditions | Kinetics equation of degradation | Rate constants of degradation | | |
|---|---|---|---|---|
| | | $R^2$ | $K$ (day$^{-1}$) | $T_{1/2}$ (days) |
| Zero order | | | | |
| InP + *C. tropicalis* NN4 | $C_t = -0.0434t + 1.008$ | 0.9631 | 0.0434 | 11.521 |
| InP + *C. tropicalis* NN4 + produced biosurfactant | $C_t = -0.0458t + 0.996$ | 0.9673 | 0.0458 | 10.917 |
| InP + *C. tropicalis* NN4 + Fe nanoparticles (0.008 g L$^{-1}$) | $C_t = -0.0522t + 0.994$ | 0.9785 | 0.0522 | 9.578 |
| InP + *C. tropicalis* NN4 + produced biosurfactant + Fe nanoparticles (0.008 g L$^{-1}$) | $C_t = -0.0544t + 0.983$ | 0.9815 | 0.0544 | 9.191 |
| First order | | | | |
| InP + *C. tropicalis* NN4 | $\ln C_t = -0.0669t + 0.493$ | 0.9650 | 0.0669 | 9.914 |
| InP + *C. tropicalis* NN4 + produced biosurfactant | $\ln C_t = -0.0741t + 0.431$ | 0.9727 | 0.0741 | 9.352 |
| InP + *C. tropicalis* NN4 + Fe nanoparticles (0.008 g L$^{-1}$) | $\ln C_t = -0.096t + 0.0759$ | 0.9795 | 0.0960 | 7.218 |
| InP + *C. tropicalis* NN4 + produced biosurfactant + Fe nanoparticles (0.008 g L$^{-1}$) | $\ln C_t = -0.107t + 0.0813$ | 0.9837 | 0.1070 | 6.477 |
| Second order | | | | |
| InP + *C. tropicalis* NN4 | $1/C_t = 0.11t + 0.8634$ | 0.9544 | 0.11 | 9.091 |
| InP + *C. tropicalis* NN4 + produced biosurfactant | $1/C_t = 0.1299t + 0.846$ | 0.9596 | 0.1299 | 7.698 |
| InP + *C. tropicalis* NN4 + Fe nanoparticles (0.008 g L$^{-1}$) | $1/C_t = 0.2037t + 0.6763$ | 0.9341 | 0.2037 | 4.909 |
| InP + *C. tropicalis* NN4 + produced biosurfactant + Fe nanoparticles (0.008 g L$^{-1}$) | $1/C_t = 0.252t + 0.5734$ | 0.9191 | 0.2520 | 3.968 |

## Kinetic studies

The kinetic data on degradation of InP (1 mg L$^{-1}$) were best fitted with the first-order kinetic model in case of all set of conditions. The highest regression coefficient ($R^2$) values of (0.9837) of InP degradation was noted in case of biosurfactant-producing *C. tropicalis* NN4 in presence of Fe nanoparticles as shown in Table 2. The calculated degradation rate constant ($K$) of InP is 0.107 day$^{-1}$ and the theoretical half-life of InP is 6.477 days implied that the removal of InP by yeast strain was a time-dependent process and degradation rate was directly proportional to substrate concentration (Jin et al. 2017).

## Conclusion

To conclude, a sophorolipid biosurfactant was produced by *C. tropicalis* NN4 which could enhance the degradation of indeno(1,2,3-cd)pyrene (InP) in the growth medium. However, the best improvement on InP degradation evaluated to 79 ± 0.05% was recorded in the presence of both biosurfactant and Fe nanoparticles. In addition, statistical optimization of growth parameters remarkably enhanced the InP degradation (90%) by *C. tropicalis* NN4 in the presence of Fe nanoparticles and produced biosurfactant which establishes the novelty of our work. Results suggested the potential applicability of the selected yeast *C. tropicalis* NN4 for the bioremediation of InP-contaminated sites using biosurfactant and specific concentration of Fe nanoparticles. To the best of our knowledge, this is the first report on nanobioremediation of InP, a high-molecular weight PAH using *C. tropicalis* NN4.

**Acknowledgements** The authors are grateful to VIT, Vellore, for providing necessary laboratory facilities.

## Compliance with ethical standards

**Conflict of interest** The authors declare no conflict of interest.

## References

Agarry SE, Aremu MO, Aworanti OA (2013) Kinetic modelling and half-life study on enhanced soil bioremediation of bonny light crude oil amended with crop and animal-derived organic wastes. J Pet Environ Biotechnol 4:137–147

Awwad AM, Salem NM (2012) A green and facile approach for synthesis of magnetite nanoparticles. Nanosci Nanotechnol 6:208–213

Bhattacharya S, Das A, Prashanthi K, Palaniswamy M, Angayarkanni J (2014) Mycoremediation of benzo [a] pyrene by *Pleurotus ostreatus* in the presence of heavy metals and mediators. 3 Biotech 4:205–211

Bodour AA, Miller-Maier RM (1998) Application of a modified drop-collapse technique for surfactant quantitation and screening of biosurfactant-producing microorganisms. J Microbiol Methods 32:273–280

Bodour AA, Gerrero-Barajas C, Maier M (2004) Structure and characterization of flavolipids, a novel class of biosurfactant produced by *Flavolipid* sp. strain MTN11. Appl Environ Microbiol 10:1114–1120

Boz N, Degirmenbasi N, Kalyon DM (2009) Conversion of biomass to fuel: transesterification of vegetable oil to biodiesel using KF loaded nano-$\gamma$-$Al_2O_3$ as catalyst. Appl Catal B 89:590–596

Capellos C, Bielski BH (1972) Kinetic systems: mathematical description of chemical kinetics in solution. Wiley-Inter science, New York

Chaki SH, Malek TJ, Chaudhary MD, Tailor JP, Deshpande MP (2015) Magnetite $Fe_3O_4$ nanoparticles synthesis by wet chemical reduction and their characterization. Adv Nat Sci Nanosci Nanotechnol 6:035009

Chandran P, Das N (2012) Role of sophorolipid biosurfactant in degradation of diesel oil by *Candida tropicalis*. Biorem J 16:19–30

Devatha CP, Thalla AK, Katte SY (2016) Green synthesis of iron nanoparticles using different leaf extracts for treatment of domestic waste water. J Clean Prod 139:1425–1435

Du Y, Dou J, Cheng L, Ding A, Fan F, Chen H (2010) Biodegradation of indeno(1,2,3-cd)pyrene by a pure bacterial culture of *Pandoraea* sp. In: iCBBE, 4th international conference on IEEE, pp 1–4

El-Sheshtawy HS, Ahmed W (2017) Bioremediation of crude oil by *Bacillus licheniformis* in the presence of different concentration nanoparticles and produced biosurfactant. IJEST 14:1603–1614

Folch J, Lees M, Sloane-Stanley GH (1957) A simple method for the isolation and purification of total lipids from animal tissues. J Biol Chem 226:497–509

Haghighat S, Akhavan A, Assadi MM, Pasdar SH (2008) Ability of indigenous *Bacillus licheniformis* and *Bacillus subtilis* in microbial EOR. Int J Environ Sci Technol 5:385–390

Huang R, Tian W, Yu H (2015) Enhanced biodegradation of HMW-PAHs using immobilized microorganisms in an estuarine reed wetlands simulator. In: IPEMEC, pp 1151–1154

Ibrahim HMM (2018) Characterization of biosurfactants produced by novel strains of *Ochrobactrum anthropi* HM-1 and *Citrobacter freundii* HM-2 from used engine oil-contaminated soil. Egypt J Pet 27:21–29

Jianlong W, Xiangchun Q, Liping H, Yi Q, Hegemann W (2002) Microbial degradation of quinolone by immobilized cells of *Burkholderia pickettii*. Water Res 36:2288–2296

Jin X, Tian W, Liu Q, Qiao K, Zhao J, Gong X (2017) Biodegradation of the benzo[*a*]pyrene-contaminated sediment of the Jiaozhou Bay wetland using *Pseudomonas* sp. immobilization. Mar Pollut Bull 117:283–290

Khopade A, Ren B, Liu XY, Mahadik K, Zhang L, Kokare C (2012) Production and characterization of biosurfactant from marine *Streptomyces* species B3. J Colloid Interface Sci 367:311–318

Klačanová K, Fodran P, Šimon P, Rapta P, Boča R, Jorík V et al (2013) Formation of Fe(0)-nanoparticles via reduction of Fe(II) compounds by amino acids and their subsequent oxidation to iron oxides. J Chem 10:961629

Korda APAR, Santas P, Tenente A, Santas R (1997) Petroleum hydrocarbon bioremediation: sampling and analytical techniques, in situ treatments and commercial microorganisms currently used. Appl Microbiol Biotechnol 48:677–686

Kumar AP, Janardhan A, Viswanath B, Monika K, Jung JY, Narasimha G (2016) Evaluation of orange peel for biosurfactant production by *Bacillus licheniformis* and their ability to degrade naphthalene and crude oil. 3 Biotech 6:43

Lawal AT (2017) Polycyclic aromatic hydrocarbons. A review. Cogent Environ Sci 3:1339841

Lowry OH, Rosebrough NJ, Farr AL, Randall RJ (1951) Protein measurement with the Folin phenol reagent. J Biol Chem 193:265–275

Luo F, Yang D, Chen Z, Megharaj M, Naidu R (2015) One-step green synthesis of bimetallic Fe/Pd nanoparticles used to degrade Orange II. J Hazard Mater 303:145–153

Makarov VV, Makarova SS, Love AJ, Sinitsyna OV, Dudnik AO, Yaminsky IV, Taliansky ME, Kalinina NO (2014) Biosynthesis of stable iron oxide nanoparticles in aqueous extracts of *Hordeum vulgare* and *Rumex acetosa* plants. Langmuir 30:5982–5988

Mantsch HH, Chapman D (1996) Infrared spectroscopy of biomolecules. Wiley-Liss

Mnif I, Sahnoun R, Ellouz-Chaabouni S, Ghribi D (2017) Application of bacterial biosurfactants for enhanced removal and biodegradation of diesel oil in soil using a newly isolated consortium. Process Saf Environ Prot 109:72–81

Mueller-Spitz SR, Crawford KD (2014) Silver nanoparticle inhibition of polycyclic aromatic hydrocarbons degradation by *Mycobacterium* species RJGII-135. Lett Appl Microbiol 58:330–337

Ooi BG, Mulisa A, Kim HY, Chong NS (2003) Methods development for the detection of trace metabolites from the biodegradation of polycyclic aromatic hydrocarbons by yeasts. J Tenn Acad Sci 78:65–75

Ping L, Zhang C, Cui H, Yuan X, Cui J, Shan S (2017a) Characterization and application of a newly isolated pyrene-degrading bacterium, *Pseudomonas monteilii*. 3 Biotech 7:309

Ping L, Guo Q, Chen X, Yuan X, Zhang C, Zhao H (2017b) Biodegradation of pyrene and benzo [a] pyrene in the liquid matrix and soil by a newly identified *Raoultella planticola* strain. 3 Biotech 7:56

Prasad KS, Gandhi P, Selvaraj K (2014) Synthesis of green nano iron particles (GnIP) and their application in adsorptive removal of As (III) and As (V) from aqueous solution. Appl Surf Sci 317:1052–1059

Sahoo C, Gupta AK (2012) Optimization of photocatalytic degradation of methyl blue using silver ion doped titanium dioxide by combination of experimental design and response surface approach. J Hazard Mater 215:302–310

Satpute SK, Bhawsar BD, Dhakephalkar PK, Chopade BA (2008) Assessment of different screening methods for selecting biosurfactant producing marine bacteria. Ind J Mar Sci 37:243–250

Satpute SK, Banpurkar AG, Dhakephalkar PK, Banat IM, Chopade BA (2010) Methods for investigating biosurfactants and bioemulsifiers: a review. Crit Rev Biotechnol 30:127–144

Shin KH, Cha DK (2008) Microbial reduction of nitrate in the presence of nanoscale zero-valent iron. Chemo 72:257–262

Spiro RG (1966) Analysis of sugars found in glycoproteins. In: Neufeld EF, Ginsburg V (eds) Methods in enzymology. Academic Press, vol 8, pp 3–26

Su X, Bamba AM, Zhang S, Zhang Y, Hashmi MZ, Lin H, Ding L (2018) Revealing potential functions of VBNC bacteria in polycyclic aromatic hydrocarbons (PAHs) biodegradation. Lett Appl Microbiol 66:277–283

Thavasi R, Nambaru VS, Jayalakshmi S, Balasubramanian T, Banat IM (2009) Biosurfactant production by *Azotobacter chroococcum* isolated from the marine environment. Mar Biotechnol 11:551

Wang T, Jin X, Chen Z, Megharaj M, Naidu R (2014) Green synthesis of Fe nanoparticles using eucalyptus leaf extracts for treatment of eutrophic wastewater. Sci Total Environ 466:210–213

Zhang X, Zhang N, Fu H, Chen T, Liu S, Zheng S, Zhang J (2017) Effect of zinc oxide nanoparticles on nitrogen removal, microbial activity and microbial community of CANON process in a membrane bioreactor. Bioresource Technol 243:93–99